UCID- 20343

A Physics Overview of AVLIS

Richard W. Solarz

February 1985

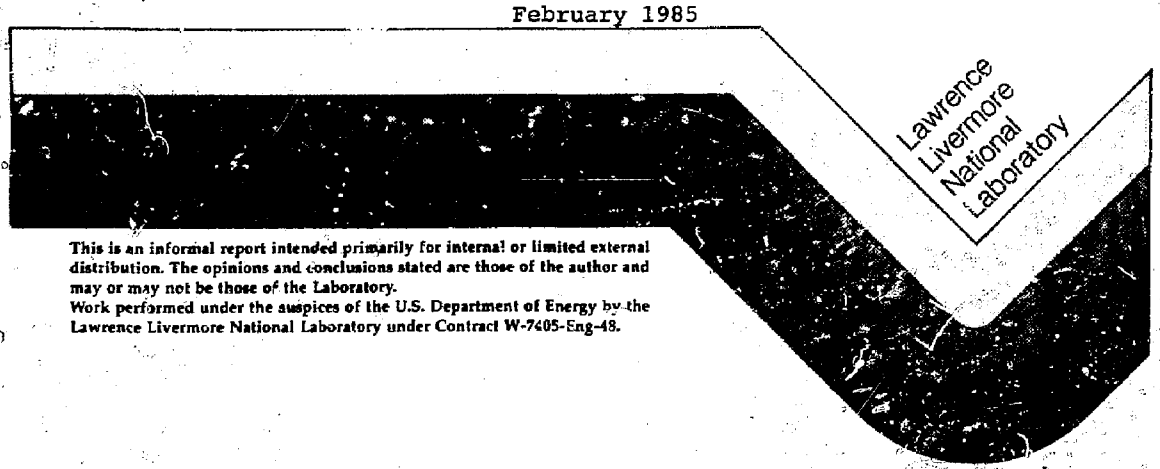

A PHYSICS OVERVIEW OF AVLIS

UCID--20343

DE85 014854

Richard W. Solarz

Atomic vapor laser isotope separation (AVLIS) represents the largest-scale potential application of tunable lasers that has received serious attention within the chemical physics community. For over a decade the U.S. Department of Energy has funded an aggressive program in AVLIS at Lawrence Livermore National Laboratory. After extensive research, the underlying physical principles have been identified and optimized, the major technology components have been developed, and the integrated enrichment performance of the process has been tested under realistic conditions. In this report, we will attempt to outline the central physical processes, review progress to date on the technology elements, and formulate scaling laws that can be used to scope out new applications.

The two primary applications of major interest to the Department of Energy are the production of light-water reactor fuel and the conversion of fuel-grade plutonium to weapons-grade material. In FY84 the total AVLIS funding level for these two missions was approximately $150M. In addition to these primary missions, a variety of applications exist that all potentially use a common base of AVLIS technology. These include missions such as the enrichment of mercury isotopes to improve fluorescent lamp efficiency, the enrichment of iodine isotopes for medical isotope use, and the cleanup of strontium from defense waste for recovering strontium isotopes for radio-thermal mechanical generators. We will see that the ability to rapidly assess the economic and technical feasibility of each mission is derived from the general applicability of AVLIS physics and AVLIS technology.

OVERVIEW OF THE AVLIS APPROACH

The only requirements that need to be met so AVLIS will be technically feasible for a particular mission are:

- The material must be able to be generated in atomic form.
- The ionization potential should be, but need not be, modest (~10 eV).
- The isotopes of the element of interest must have an isotope shift resolvable by some spectroscopic method (these shifts need not be greater than an atomic Doppler-broadened line width).

Rapid deployment of a given mission would require that it use the copper-vapor-laser-pumped dye laser technology developed at Livermore and, for refractory materials, require that electron beam based metal vapor sources be used.

In AVLIS the feedstock is normally contained in a crucible and is heated from above by an electron beam to temperatures sufficient to generate a substantial vapor pressure of material from the surface of the electron-beam-heated melt. The gas-phase atoms are initially in temperature equilibrium with the surface and the internal temperature of the atom is often several thousands of degrees. At these temperatures, very complex atoms (transitions metals, actinides, lanthanides) have only a small fraction of the atoms with no internal electronic excitation. Fortunately, by the process of atom-atom collisions, the energy initially contained in the electronic degree of freedom is transferred to the translational degrees of freedom, resulting in a cooling of the internal temperature of the atoms and simultaneously resulting in a highly directed motion of the flow of the material. The process is quite similar to the relaxation process that takes place in nozzled beams and will be elaborated upon later. The important result is that even refractory materials ionized by electron beams can be configured to deliver low internal temperature atomic vapor.

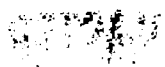

Since much or most of the material is in the lowest-lying electronic state, a single frequency of light can be used to excite the isotope of interest. Figure 1 shows a typical absorption spectrum of a heavy element. It also shows that isotopes can be selectively photoionized using polarization selection rules even when isotope shifts are small. For heavy atoms where the isotope shift is dominated by the nuclear volume shift, or for the light elements in which it is dominated by the specific mass effect, the precise absorption frequency difference for the isotopes is in general larger than the absorption line width. This absorption line width in the visible region of the electromagnetic spectrum is dominated by either the Doppler effect or hyperfine structure for some isotopes. Again, the richness of the spectra of the heavy elements generally gives us the luxury of selecting an excitation frequency that has small hyperfine dispersion. As a result, selective excitation of the isotope of interest can be assured.

After the generation of the vapor and the selective excitation of one or more of its components, all that remains is to preferentially remove from the flow stream, by one of several methods, the excited material. The excited atoms may be such that they rapidly undergo chemical reactions with a covaporized material and the resultant low vapor pressure product may preferentially condense from the stream (photochemical approach). Another method may be to use additional lasers to further excite the isotopes until they ionize, either by the process of direct photoionization, collisional ionization, or by field ionization (photophysical approaches). Figure 2 shows some candidate photoionization approaches that use the fundamental wavelengths or harmonics of the dye lasers excited by our baseline copper-vapor-laser-pumped dye lasers. The vast majority of the atoms in the periodic table can be accessed by these lasers (Fig. 3).

Concentrating on the photophysical separation approach, we return to removing the ions of isotope A from the neutral atoms in the flow. This can be arranged by the application of suitable voltages to structures placed near the flow. The ions are attracted to the negatively charged structures while the neutrals continue unimpeded in their flow until they

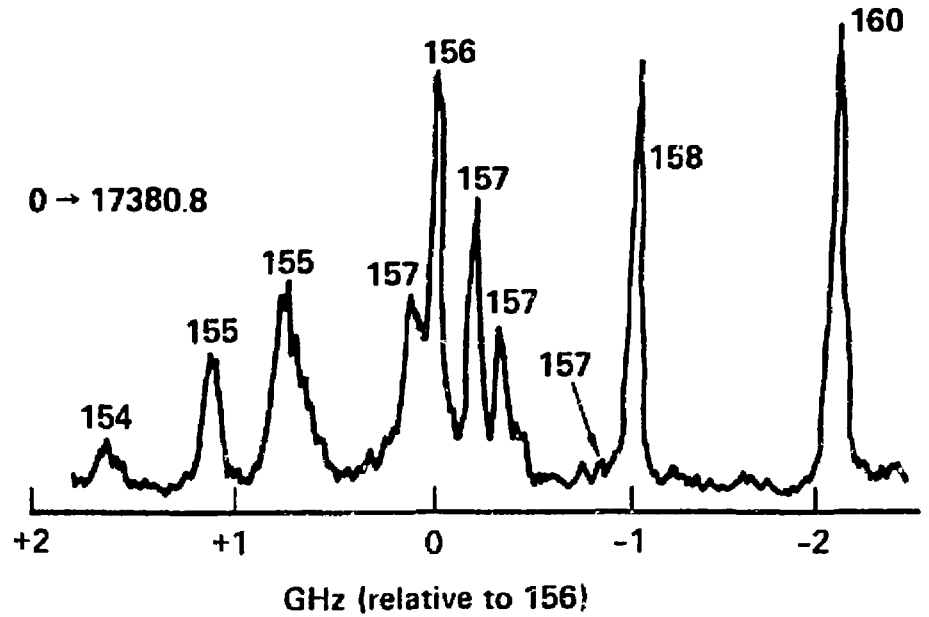

Fig. 1. An example of Gd absorption profiles in an atomic beam.

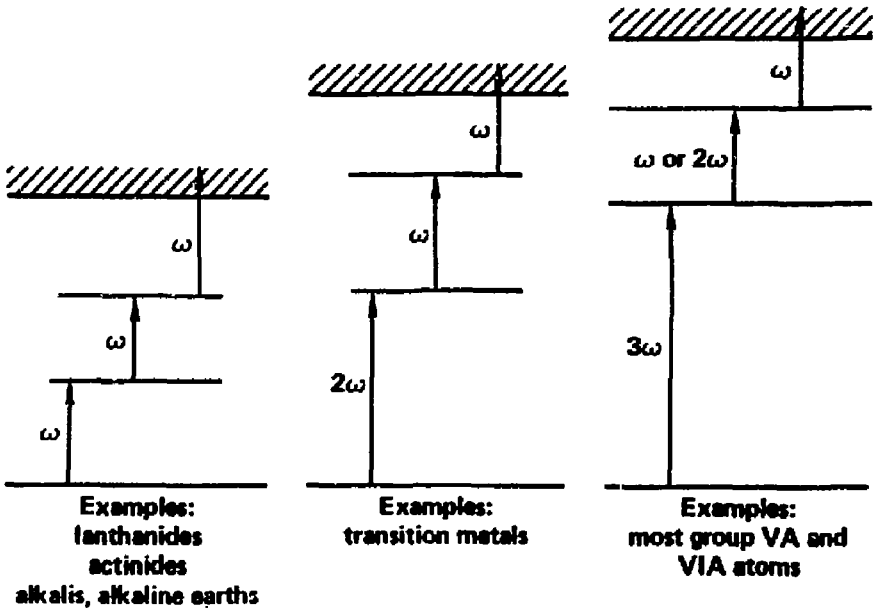

Fig. 2. Sample AVLIS excitation pathways.

condense onto a plate placed directly above the source (Fig. 4). The process is now complete with the material that has been laser photo-excited and ionized remaining on the extractor structures. The unexcited component flows to the collector plate.

Figure 4 gives an overview of the entire separation process. In this figure the extractor is labeled as the product collector and the collector is labeled as the tails collector. The performance of the entire process can be measured by either of two sets of variables β_1 and β_2 or η and ϕ, which are simply related to one another as shown in the figure. The variables β_1 and β_2 are referred to as the enrichment and depletion factors and are the standard measures of performance in the enrichment industry. Roughly, they measure the change in assay of the product and tails material from that of the initial feed. The variables η and ϕ are more directly related to the physics of the process. They measure, respectively, the stripping efficiency (the fraction of desired isotopes stripped from the feed in a single pass) and the nonselective pickup (the fraction of the feed material that plates out on the extractor in the absence of light). The latter process is caused by many distinct processes but is generally dominated by the aerodynamic coating out of the imperfectly directed flow stream onto the extractor structures.

The stripping efficiency and nonselective pickup are fundamental in that they determine whether a process needs to be staged in order to achieve specific enrichment goals. They also determine the fraction of the feed stream that is usefully converted to product. The stripping efficiency can be calculated essentially by the the simple multiplication of three factors:

- f_a, the fraction of atomic material available in the ground electronic state that can be excited by the lasers.
- f_i, the fraction of the ground electronic state atoms that can be ionized by a finite amount of delivered laser power.
- f_c, the fraction of the ionized isotopes that are collected.

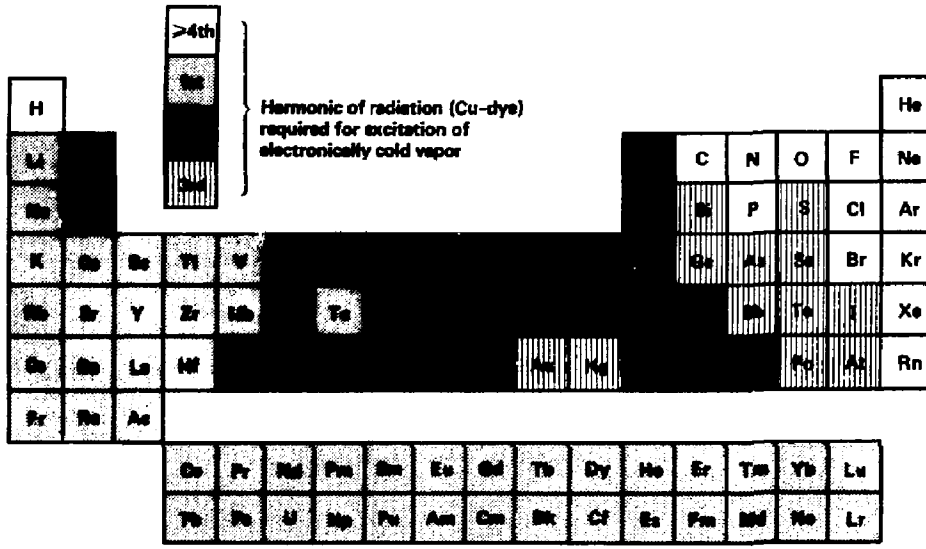

Fig. 3. Elements separable by AVLIS using copper laser/dye laser technology.

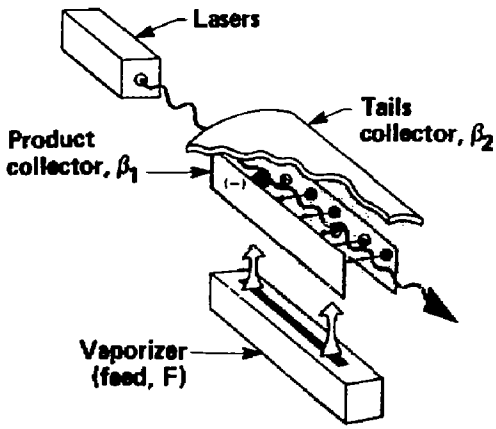

$$\beta_1 = 1 - \eta_S + \frac{\eta_S}{\phi}$$

$$\beta_2 = \frac{1}{1-\eta_S}$$

Separative work depends only upon

β_1 = Enrichment factor		η_S = Stripping efficiency	
β_2 = Depletion factor	OR	ϕ = Non-selective pickup	
τ = Throughput		τ = Throughput	

Fig. 4. AVLIS concept: alternative separation parameters.

Figure 5 shows a chart of these factors. Taken together, Fig. 6 shows that η and ϕ can be preselected to yield the desired product assay of a given process. High selectively assumes high-purity products. In general, it is feasible to achieve enrichment factors in excess of 10 and near 100 in a practical working device.

PHYSICS OF THE AVLIS PROCESS

AVLIS is a converging point for many fields of physics and draws heavily on understanding from plasma physics, aerodynamics, conventional and nonlinear spectroscopy, surface physics, kinetics, and many other disciplines. We will outline in somewhat more satisfying terms the extent to which each physical effect determines the performance of an AVLIS separator.

The physical processes that are included in the atomic expansion are summarized in Fig. 7. Starting with the source at the bottom, we assure that the melt surface temperature is known from the source characteristic. (This assumption is verified by comparing the energy content of the flow with measured values.) Within several mean free paths above the melt surface, the velocity distribution of the vapor atoms evolves from a single-sided distribution into one with an isotropic random-velocity componert superimposed on a bulk drift velocity. An available solution of the Boltzmann equation is used to describe this flow reorganization and to fix the boundary condition for the gas-dynamic equations. The heating of the vapor as it passes through the electron beam is calculated from a kinetic equation. The variation of vapor properties (atom density n, translational temperature T, isotropic Mach number m, and bulk flow velocity V_f) is determined by solving the one-dimensional gas-dynamic equations in a given stream tube, coupled with the rate equations characterizing electronic energy transfer of the vapor. Near the extractor the density of the vapor has dropped far enough that collisions become rare.

The rate equations that close the system of equations describing the vapor expansion deal with the finite rate of energy transfer to and from the electronic states of the vapor. Guided by experimental evidence, we

- **Definition**

  η_s = fraction of atoms ionized by lasers and collected as product

- **Controlling physics**

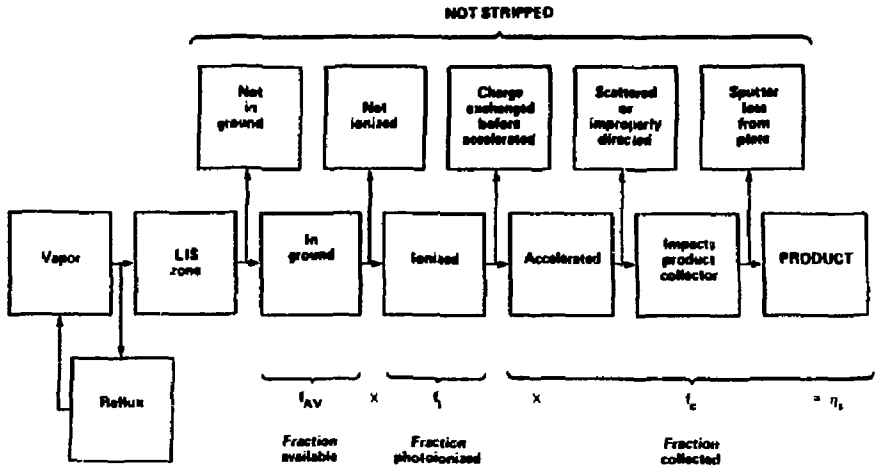

Fig. 5. Stripping efficiency.

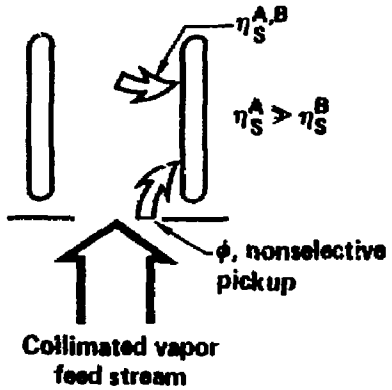

$$\chi_A^P = \left[\frac{\frac{\eta_S^A}{\phi} + (1 - \eta_S^A)}{\frac{\eta_S^B}{\phi} + (1 - \eta_S^B)}\right] \chi_A^F$$

For example:

$\eta_S^B = 0.5\%$, $\phi = 1\%$, $\chi_A^F = 1\%$, $\eta_S^A = 75\%$

$\chi_A^P > 50\%$

- In general η_S^A/η_S^B and ϕ are designed to yield desired χ_A^P.
- High selectivity ($\eta_S^A/\eta_S^B \gg 1$) in AVLIS assures high purity product in minimum number of stages.

Fig. 6. Product purity considerations in AVLIS.

describe the population and thus the energy of the electronically excited atoms by a single parameter, the internal temperature T_i. Within the framework of a continuum description of the flow, the energy associated with the random translational motion of the atoms is also characterized by a single parameter, the translational temperature T. The energy flow in the expansion is represented in Fig. 8. The vapor starts with an energy determined by the surface temperature of the melt. The electronic energy of the vaporized atoms is assumed to be equal to the equilibrium internal (electronic) energy of atoms at the surface temperature. The vaporized atoms also carry translational energy, which is lower than the equilibrium value at the surface temperature because of the single-sided velocity distribution. We treat the electronic energy of the vapor separately from the translational energy, since the former does not participate directly in the aerodynamics of the flow.

The electronic states of the vapor are also heated by collisions with the high-energy (15 to 45 keV) electrons in the electron beam. The amount of heating is calculated by integrating the Berger-Seltzer values for electron-beam energy loss along the trajectories of the incident and skip beams. We assume that a fraction (C_2) of the electron-beam energy loss remains in the vapor as internal excitation. Figure 9 gives example relative energy sources and energy distributions for fixed collector distances for a typical feed material (gadolinium) that has been electron-beam vaporized. The resultant internal electronic temperature of the material vaporized from a 2500 K melt surface was 800 ± 200 K at a 25-cm distance from the melt. The mach number M was 5.0. The resulting fraction available is 0.5 and the non-selective pickup can be arranged to have a variety of values depending upon the arrangement of the collector assembly.

A detailed understanding of the structure of atom is the starting point for all AVLIS process photoionization designs. Identification of the electronic levels is necessary for the determination of optimum laser wavelengths for AVLIS processes. The hyperfine structure of the atoms is vital to the design of multistep AVLIS because the fraction of ground-state uranium ionized, and thus the system throughput, is sensitive to the degree to which the individual hyperfine components are

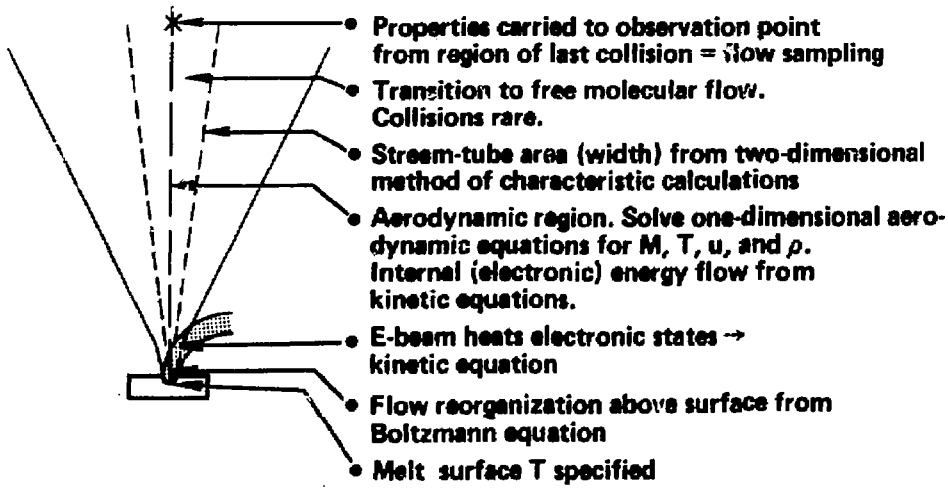

Fig. 7. Processes considered in 1-dimensional model: SLEW code.

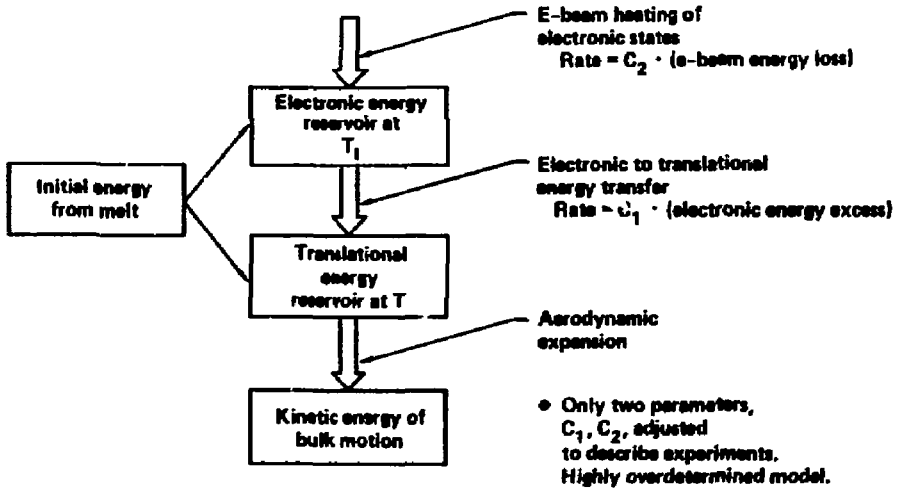

Fig. 8. Energy flows in vapor expansion.

accessed. Level lifetimes must be measured so that radiative decay losses during the laser excitation process can be accounted for and minimized. Isotope shifts are required so that process selectivity can be assessed for a variety of multistep excitation pathways. Excitation cross sections are needed so that the required laser power for plant modules can be determined. Also, precise measurements of cross sections are necessary to establish the plant laser power requirements. They also permit us to use these well known parameters as a diagnostic for vapor-source performance. Many of these parameters, such as isotope shifts, cross sections, and hyperfine structure, are also critical to the assessment of a variety of laser-beam propagation phenomena.

Figures 10 and 11 show typical bound-bound absorption cross-section data for a heavy atom (uranium) and typical autoionization spectra for another heavy atom (dysprosium). Typical bound-bound and autoionization cross sections of heavy elements are seen to be in the range of 10^{-14} cm^2 and 10^{-16} cm^2, respectively. As a result, these transitions can be saturated with typically millijoules per cm^2 or less fluence per pulse. A detailed model has been constructed to predict the ionization vs fluence behavior for multistep excitation-ionization processes. The atomic parameters input into the code are absorption cross sections, hyperfine structure, line width, lifetimes, and isotope shifts. The laser field is accurately represented by inputing the temporal, spatial, polarization, and frequency behavior. Typical measured saturation behavior for a three-step photoionization process in a heavy element is shown in Fig. 12. The important point is that infinite fluence will give unit ionization efficiency. More realistic and economic laser fluence can easily yield reasonably high f_i values. Depending upon the exact stripping efficiency required for a given mission, laser power can be traded off for ionization to achieve the optimum economic process design.

The extraction process can also be configured to yield a fraction collected up to near unity. The principal physical mechanism that limits the extraction process is usually charge exchange. However, it is important to understand that resonant charge exchange taking place after the photoions have been created does not degrade the efficiency of the

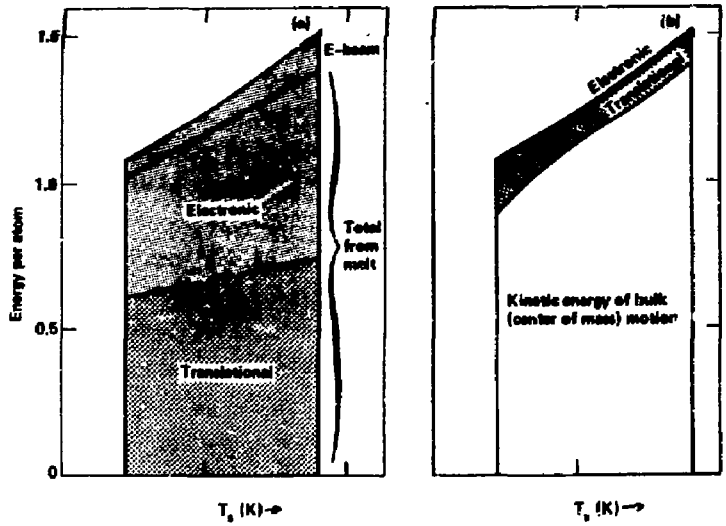

Fig. 9. Energy balance in vapor expansion.

Wavelength (Å)	Energy levels (cm^{-1})	Upper-state lifetime (ns)		gA ($10^3\ s^{-1}$)			Branching ratio
4362.1	0 (j = 6) - 22918.555 (j = 7)	This work 68 ± 10	Corliss 75	This work 1.76 ± 0.30	Voigt 2.57	Corliss 1.6	This work 0.80 ± 0.10
4393.6	0 (j = 6) - 22754.061 (j = 6)	66 ± 5	81	1.36 ± 0.20	2.12	1.2	0.65 ± 0.10

Fig. 10. Lifetime and transition probabilities in ^{238}U.

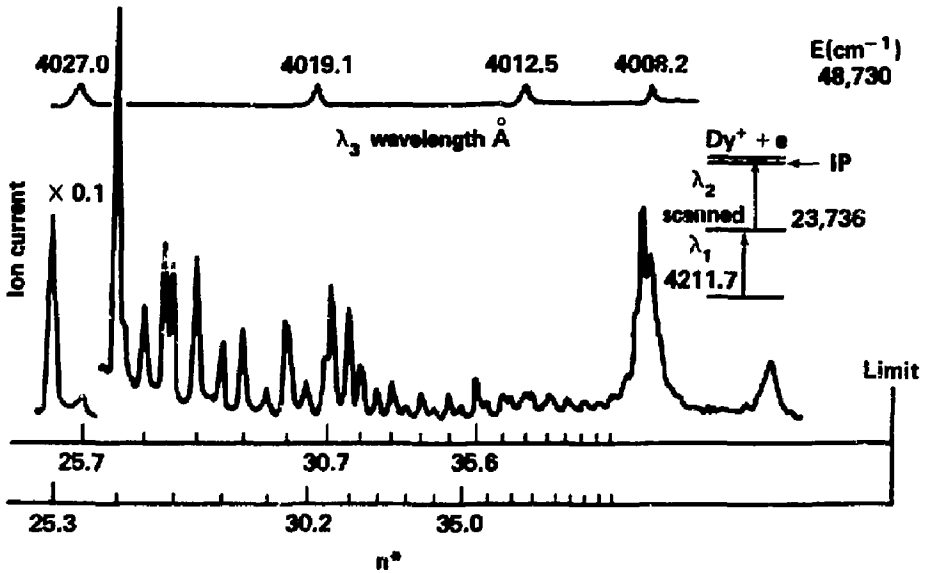

Fig. 11. Dysprosium autoionizing Rydberg series.

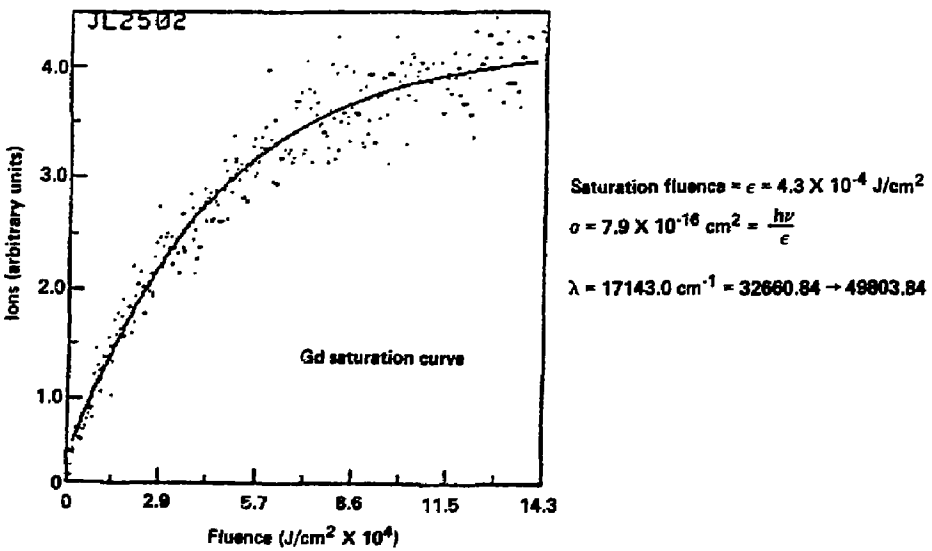

Fig. 12. Photoion Data.

process. To minimize the overall degradation of the extraction efficiency, it is usually necessary to limit the neutral density (and by implication the plasma density) to a small enough value to permit the space-charge-limited flow of ions through the plasma sheath on a time scale before resonant charge exchange within the body of the plasma becomes significant.

In general we thus see that the overall stripping efficiency of the AVLIS process can be typically:

$$\eta = f_a \times f_i \times f_c \sim 0.5 \quad . \tag{1}$$

If higher values are needed, laser power can be increased to improve f_i, plasma density can be reduced to increase f_c, work can be invested to improve f_a, or all three approaches can be invested in simultaneously.

STATUS OF AVLIS TECHNOLOGY DEVELOPMENT

The sustained support of the U.S. Department of Energy for the development of AVLIS technology since 1973 and the commonality of the physical elements of the technology for a wide range of feedstocks have permitted rapid development of the necessary components. During the past 5 years we have obtained substantial operating experience on laser systems that deliver nominally 100 W of tunable dye laser light. Our separator systems have operated repeatedly at nominally full scale for periods in excess of 100 hours and have demonstrated the ability to reliably generate and collect material under realistic operating conditions. A continuing series of integrated enrichment tests has demonstrated the ability of the completed systems subassemblies to interface reliably to generate the predicted enrichment of feeds under operating conditions identical to those of a plant.

The AVLIS program at LLNL is currently involved in an aggressive construction program in its 85,000 ft^2 special isotope separation laboratory (SISL, Fig. 13). A very large laser system and separator are being installed (Figs. 14 to 16), which will initially deliver in excess

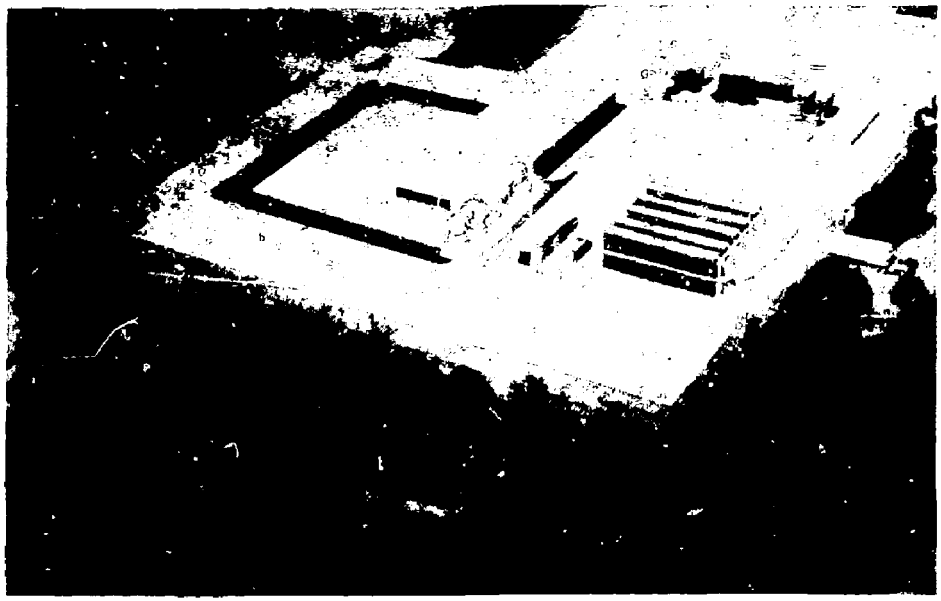

Fig. 13. Special Isotope Separation Laboratory (SISL).

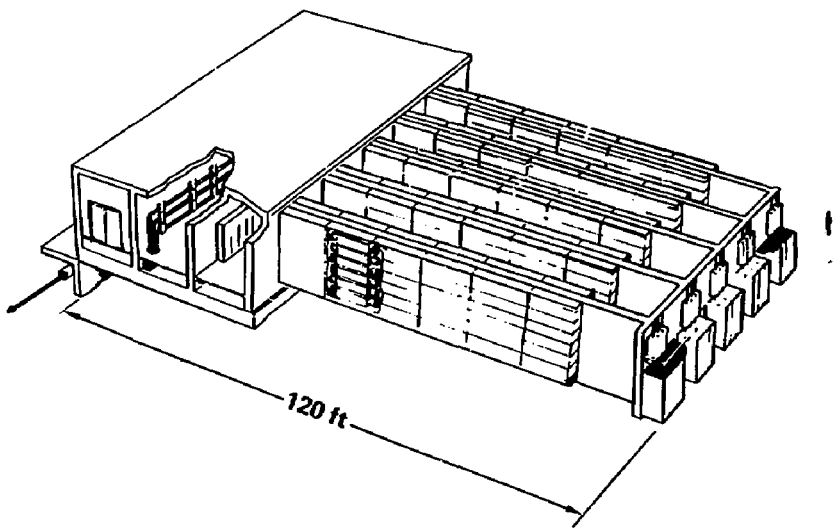

Fig. 14. SISL laser subsystem.

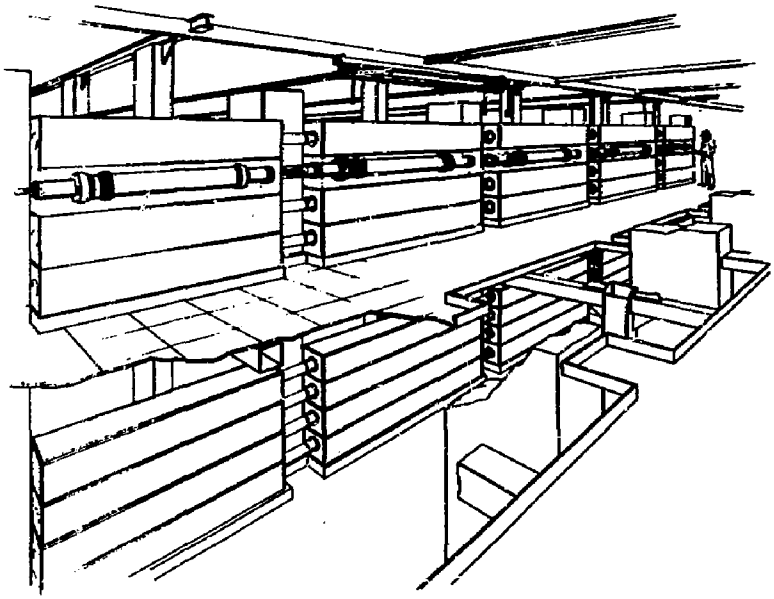

Fig. 15. Laser-demonstration facility copper-laser MOPA.

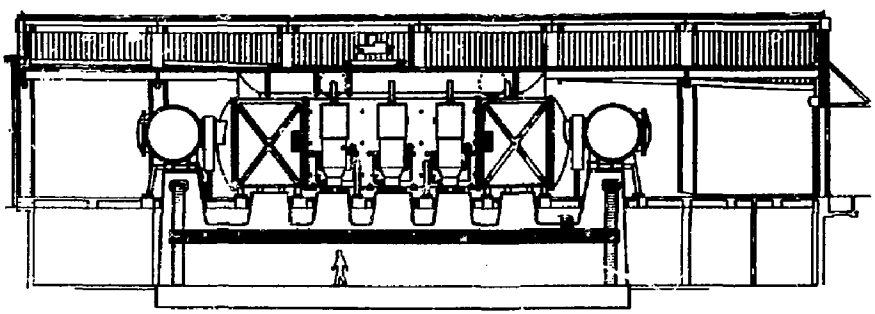

Fig. 16. Full-scale demonstration facility process chamber--high-bay elevation.

of kilowatts of tunable dye laser light and meters of uranium vapor. These systems are expected to be operational within nine months.

The laser system master-oscillator/power-amplifier (MOPA) architectural approach and the modular design and quick-disconnect features of individual laser heads make it possible to repair or quickly replace individual laser heads without disrupting the operation or performance of the overall system. Individual copper-laser heads have been constructed and operated at power in excess of 150 W of maximum extractable power (MEP) and 500-W heads will soon be demonstrated.

Similar progress has been achieved in separator technology. The ability to collect material in the solid phase (batch processes) and liquid phase (continuous processes) has been proven.

It is clear that the AVLIS process has been scaled well beyond the experimental benchtop level. This places us on the path to a commercial production plant. Work on the AVLIS process has progressed to a point where the fundamental physics and technology have been successfully demonstrated. The program is now moving from the technology evaluation through the technology demonstration phase at engineering scale.

A wide range of applications in the area of isotopic enrichment can now be scoped using this technology. The implementation of this approach to isotope enrichment will ensure an expanded range of isotopic materials for research and commercial use.